



Effect of phenyl sepharose ligand density on protein monomer/aggregate purification and separation using hydrophobic interaction chromatography

Justin T. McCue*, Philip Engel, Jörg Thömmes

Biogen Idec Corporation, Bioprocess Development, 14 Cambridge Center, Cambridge, MA 02142, USA

ARTICLE INFO

Article history:

Received 20 October 2008

Received in revised form

25 November 2008

Accepted 1 December 2008

Available online 7 December 2008

Keywords:

Hydrophobic interaction chromatography

Phenyl sepharose

Protein purification

Preparative chromatography

Adsorption isotherm

Ligand density

Aggregate removal

ABSTRACT

In the large-scale manufacturing and purification of protein therapeutics, multiple chromatography adsorbent lots are often required due to limited adsorbent batch sizes or during replacement at the end of the useful column lifetime. Variability in the adsorbent performance from lot to lot should be minimal in order to ensure that consistent product purity and product quality attributes are achieved when a different lot or lot mixture is implemented in the process. Vendors of chromatographic adsorbents will often provide release specifications, which may possess a narrow range of acceptable values. Despite relatively narrow release specifications, the performance of the adsorbent in a given purification process could still vary from lot to lot. In this case, an alternative use test (one that properly captures the lot to lot variability) may be required to determine an acceptable range of variability for a specific process. In this work, we describe the separation of therapeutic protein monomer and aggregate species using hydrophobic interaction chromatography, which is potentially sensitive to adsorbent lot variability. An alternative use test is formulated, which can be used to rapidly screen different adsorbent lots prior to implementation in a large-scale manufacturing process. In addition, the underlying mechanism responsible for the adsorbent lot variability, which was based upon differences in protein adsorption characteristics, was also investigated using both experimental and modeling approaches.

© 2008 Elsevier B.V. All rights reserved.

1. Introduction

Chromatography is used commonly in the biotechnology industry to purify therapeutic proteins from complex mixtures [1]. In the large-scale purification of protein therapeutics, chromatography steps are often operated in two types of modes—in bind/elute mode (in which the target protein is bound and later eluted isocratically from the adsorbent) or in a flow through fashion (in which unwanted impurities bind to the adsorbent while the target species flows through the column) [2,3]. Chromatography adsorbents are screened and selected based upon their ability to effectively remove process and product related impurities. Several types of chromatography, including affinity, ion-exchange, and hydrophobic interaction, are often implemented in a process to achieve acceptable purity levels [1–3]. The different types of chromatography exploit differences in the binding properties between the target product and both process and product related impurities present in the feed.

When operated in a bind/elute fashion, numerous impurity species may co-adsorb with the target product. The impurity

species that co-adsorb must be separated from the target species, desorbed either with the use of a wash step (prior to product elution) or remain bound to the adsorbent after the target species is eluted. The binding properties of product related impurity species, such as undesirable isoforms or aggregate species, are often highly similar to the desired product [3,4], which makes the chromatographic separation more challenging. Slight changes in processing conditions or adsorbent binding properties could significantly change the ability to separate two closely related species [4]. When selecting chromatography adsorbents to perform the described separations, it is critical that lot to lot variability be minimal to ensure a consistent and predictable purification process in a large-scale manufacturing environment. In the event that adsorbent lot variability does exist, it is important that a test be available to properly screen adsorbent lots prior to implementation in manufacturing. Such a test will ensure the specific adsorbent lot provides acceptable performance.

Hydrophobic interaction chromatography (HIC) is commonly used to separate monomer and aggregate species in the purification of protein therapeutics [5–7]. Despite being an effective step for separating monomer and aggregate species, the performance of HIC can potentially be sensitive to small changes in the operating conditions and adsorbent binding properties [8–16]. Slight changes to the protein column loading or the eluate buffer salt concentration can result in an undesirable

* Corresponding author. Tel.: +1 617 679 3500; fax: +1 617 679 3408.
E-mail address: Justin.mccue@biogenidec.com (J.T. McCue).

change in the aggregate removal and yield [17–20]. Additionally, slight changes to the adsorbent binding properties could also potentially alter the separation performance of the HIC column [19–21]. The separation mechanism of a monomer and aggregate protein therapeutic species has been modeled previously using Phenyl Sepharose Fast Flow as the HIC adsorbent [22]. A model sensitivity analysis showed that relatively small changes to the absorptive properties of the adsorbent could potentially have a large impact on the separation performance for the examined protein mixture. Thus, the described separation is potentially sensitive to variability with different adsorbent lots.

In this work, we evaluated the impact of different Phenyl Sepharose Fast Flow lots on the separation performance of a monomer/aggregate mixture. A model describing the separation was developed and described in detail previously [22]. The model predictions were used in conjunction with experimental results to determine the effects of different adsorbent ligand densities on the described separation. The separation performance of the adsorbent was consistent over a range of ligand densities, but varied significantly at the higher end of the evaluated range. Both product yield and aggregate removal were sensitive to changes in the adsorbent lot ligand density.

An alternative use test was evaluated, which was based upon adsorption isotherm parameters measured rapidly in batch contact experiments. The studies showed adsorbent lot variability for the described separation could only be determined under conditions used to elute the protein mixture, as the different adsorbent lots displayed comparable behavior when evaluated under binding conditions. The alternative use test could be implemented as a method to rapidly screen out different adsorbent lots and/or lot mixtures, and determine which are acceptable for use in a pre-defined manufacturing process.

2. Experimental

2.1. Materials

2.1.1. Adsorbents

Phenyl Sepharose 6 Fast Flow (catalog No. 17-0973) from GE/Healthcare (Piscataway, NJ, USA) was used as the chromatography adsorbent in the studies. Adsorbent lots that contain different ligand densities (degree of ligand substitution) ranging from 40 to 47 μmol phenyl/mL gel were evaluated in the studies (Table 1).

2.1.2. Protein solutions

A purified, recombinant fusion protein ($M_r \sim 110$ kDa) produced in a Chinese hamster ovary cell culture broth was used as the feed. Following purification using Protein A and cation exchange chromatography steps, the material consisted of approximately 80% monomer and 20% aggregate species mixture. Both the monomer and aggregated forms of the fusion protein were further purified and isolated as the individual components. The individual species were isolated using size-exclusion chromatography (HiPrep Sephacryl S-300 HR, catalog No. 17-1196-01, GE/Healthcare). For the balance of the paper, the individual purified components will be referred to as the “monomer” and “aggregate” species. A 1.6 M

ammonium sulfate stock solution was added to the protein solutions to achieve a final concentration of 0.30–1.0 M ammonium sulfate. All solutions used in the study were filtered using 0.22 μm filtration prior to the experiments.

2.1.3. Solvents and chemicals

An acetate buffered solution containing 0.05 M sodium acetate (J.T. Baker, catalog No. 3461-05, Phillipsburg, NJ, USA) + 1.0 M ammonium sulfate (J.T. Baker, catalog No. 0792-07) (pH 6) was used as the mobile phase equilibration solution for all of the experiments, unless otherwise noted. For the elution solutions, the ammonium sulfate concentration was reduced to 0.30–0.45 M ammonium sulfate. The adsorbents were cleaned and regenerated using subsequent steps of distilled water and 1.0 M sodium hydroxide (J.T. Baker, catalog No. 3722-01), respectively, before and after the experiments.

2.2. Procedures and equipment

2.2.1. Adsorption equilibrium data

Adsorption equilibrium data for the pure monomer and pure aggregate forms of the protein using the Phenyl Sepharose Fast Flow adsorbent were determined using batch contact experiments. The batch contact experiments were performed using 96 well plates (catalog No. 5052, Pall Life Science, East Hills, NY, USA). Multiple isotherms were measured simultaneously on a single plate using relatively small amounts of adsorbent and protein solution. Each well of the plate was filled with 800 μl of buffer (0.05 M sodium acetate + 0.30–1.0 M ammonium sulfate (pH 6)) containing protein concentrations ranging from 0.1 to 6.0 mg/mL. A 50 μL adsorbent slurry sample (70% (v/v) slurry) was then added to each well and agitated at room temperature for >12 h until equilibrium was reached for all of the evaluated conditions. After equilibration, the absorbance of the solution was measured at 280 nm using a Synergy 2 Multi-Detection Microplate Reader (BioTek Part No. SLFA, Winooski, VT, USA). The amount of protein adsorbed was then obtained from a material balance. It is important to note agitation of the mixture did not impact the protein stability or aggregate levels over the time required to achieve equilibrium.

2.2.2. Column chromatography

Phenyl Sepharose Fast Flow was packed into 0.66 cm I.D. glass columns (Omnifit, Rockville Center, NY, USA) with a bed height of 20 cm. An Äkta 10 Explorer chromatography system (catalog No. 18-1300-00, GE/Healthcare) was used in all of the chromatography experiments.

Following equilibration, columns were loaded with 20 mg/mL of the protein solution at a superficial velocity of 250 cm/h. The feed used in the studies consisted of 80% monomer and 20% aggregate. Following loading, the columns were washed with 3 column volumes (CVs) of equilibration buffer (1.0 M ammonium sulfate). Protein species were eluted isocratically by decreasing the ammonium sulfate concentration to 0.30–0.45 M. The eluate was collected and analyzed for monomer and aggregate content using analytical size-exclusion chromatography (TSKgel G3000 SW_{XL}, catalog No. 08541, Tosoh BioScience, Tokyo, Japan). Product yields in the eluate pool were obtained by a material balance. Following elution, columns were cleaned using 3 CVs of distilled water and 3 CVs of 1.0 M sodium hydroxide.

3. Theoretical

The modeling approaches used to describe protein adsorption and the chromatographic separation predictions using the HIC adsorbent were explained in detail by McCue et al. [22]. The model is described briefly below to provide the basic model assumptions

Table 1
Phenyl Sepharose Fast Flow adsorbent lots evaluated in the study.

Lot no.	Ligand density (μmol phenyl/mL drained gel) ^a
10012029	40
311367	42
10005436	45
303027	47

^a Ligand density values provided by GE/Healthcare.

and concepts. Further details on the modeling formulation can be found in the prior work [22].

3.1. Modeling of the equilibrium adsorption isotherm

In this model, the two species (monomer and aggregate) are assumed to bind competitively to the HIC adsorbent. A schematic of the competitive, binary adsorption process used to model the separation using phenyl sepharose, monomer species bind completely reversibly to the adsorbent and follow the classical Langmuir adsorption [23], while a fraction of the aggregate species bind irreversibly [24]. Since a fraction of the aggregate species bound irreversibly to the adsorbent, an additional term ($q_{2,irr}$) was added to the aggregate adsorption isotherm. For the case of the pure components, Eqs. (1) and (2) were used to model the equilibrium adsorption process for the pure monomer and the pure aggregate species, respectively:

$$c_1 = \frac{q_1}{K_1(q_{m1} - q_1)} \quad (1)$$

$$c_2 = \frac{q_2 + K_{2,irr}q_2(q_{m2} - q_2 - q_{2,irr})}{K_2(q_{m2} - q_2 - q_{2,irr})} \quad (2)$$

where c_1 and c_2 represent the liquid phase concentration of monomer and aggregate species, respectively. The static binding capacity and binding strength constants are represented by q_{mi} and K_i , respectively.

Determination of the adsorption isotherm parameters used in the modeling studies is described as follows. Under binding conditions (1.0 M ammonium sulfate), values for the binding strength (K_i) and static capacity (q_{mi}) constants for the pure monomer and pure aggregate species were obtained by fitting Eqs. (1) and (2), respectively, to data from batch contact experiments (described in Section 2.2.1). A two parameter fit was used to model the adsorption isotherms under binding conditions. Differences in adsorption characteristics for the examined adsorbent lots were within experimental error for both the pure monomer (Fig. 2a) and pure aggregate species (Fig. 2b), so single values for the adsorption isotherm parameters were fitted for all of the lots. Values used for the irreversible binding parameters ($K_{2,irr}$ and $q_{2,irr}$) in Eq. (2) were the same as reported previously [22] for all of the adsorbent lots, since differences in adsorption characteristics were within experimental error under strongly binding conditions (1.0 M ammonium sulfate).

Under low salt (elution) conditions (0.30–0.45 M ammonium sulfate), an alternative fitting approach was implemented (Fig. 3). A single value for the monomer static binding capacity constant (q_{m1}) was used for the different adsorbent lots at each of the examined buffer conditions. This approach was selected because use of a two parameter fitting approach for each of the individual adsorbent lots

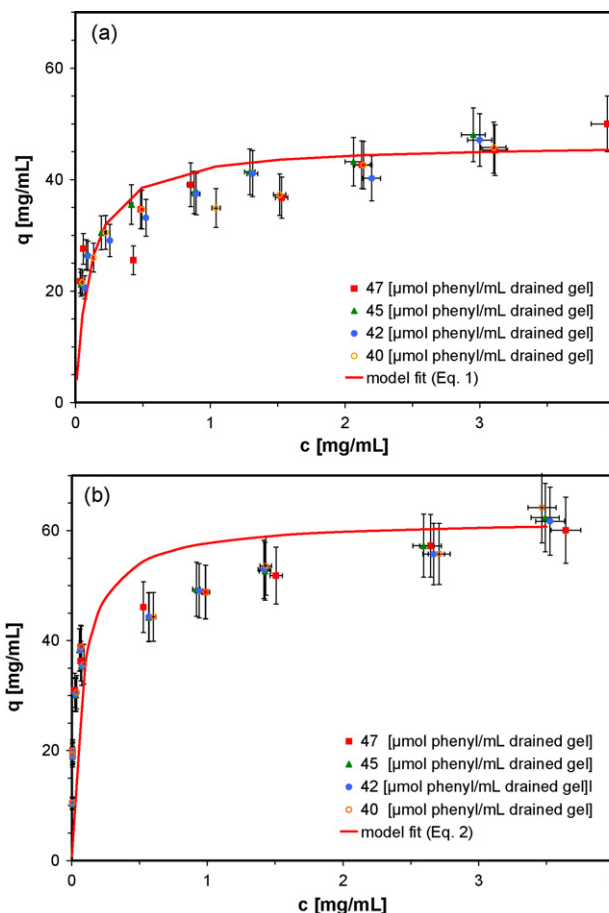


Fig. 2. Adsorption equilibrium data for pure monomer (a) and aggregate (b) species using Phenyl Sepharose Fast Flow adsorbents with different ligand densities. The liquid phase contained 1.0 M ammonium sulfate. Adsorption isotherm model fits for the monomer (Eq. (1)) and the aggregate (Eq. (2)) species are shown (solid lines). The errors bars reflect the experimental uncertainty in the measurements.

resulted in similar values for q_{m1} , which were within experimental uncertainty. After selecting a single value for q_{m1} , a best fit for Eq. (1) was then obtained for each adsorbent lot by varying the binding strength constant (K_1). Thus, the effect of adsorbent ligand density changes on monomer adsorption was quantified and captured by differences in the fitted binding strength constant (Fig. 4). Under elution conditions (0.30–0.45 M ammonium sulfate), the binding strength constant determined for the monomer species was also used for the pure aggregate species ($K_1 = K_2$) at each salt concentration for the different lots. As described by McCue et al. [22], the

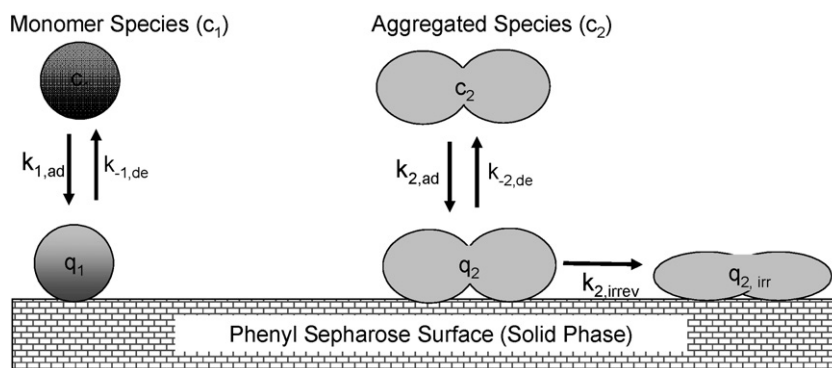


Fig. 1. Schematic of the competitive, binary adsorption process used to model the separation of a monomer and aggregate protein therapeutic mixture (from Ref. [22] with permission).

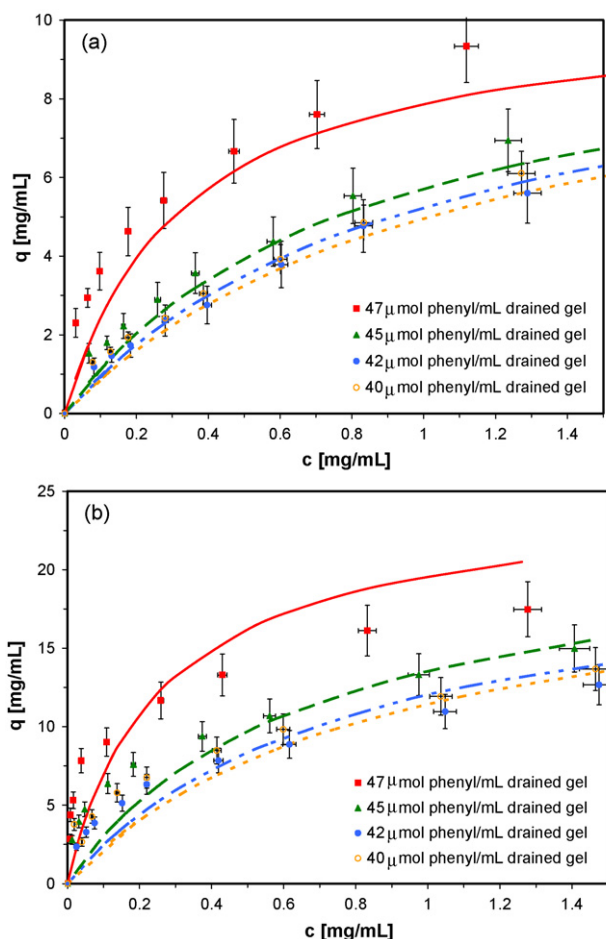


Fig. 3. Adsorption equilibrium data for pure monomer (a) and aggregate (b) species using Phenyl Sepharose Fast Flow adsorbents with different ligand densities. The liquid phase contained 0.35 M ammonium sulfate as the liquid phase. Adsorption isotherm model fits for the monomer (Eq. (1)) and the aggregate (Eq. (2)) species are shown (solid lines). The errors bars reflect the experimental uncertainty in the measurements.

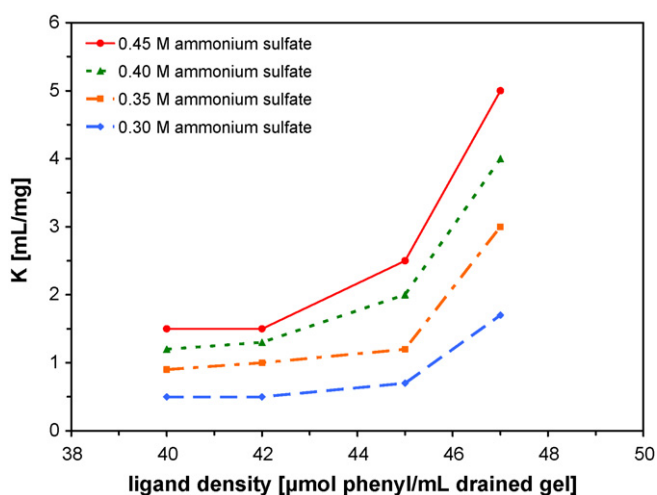


Fig. 4. Adsorption isotherm binding constants for monomer (Eq. (1)) and aggregate (Eq. (2)) species determined for Phenyl Sepharose Fast Flow adsorbents over a range of liquid phase ammonium sulfate concentrations (0.30–0.45 M). The fitted binding constants were used for both monomer (K_1) and aggregate (K_2) species.

Table 2

Fraction of irreversible bound aggregate species using different ammonium sulfate concentrations and Phenyl Sepharose Fast Flow adsorbents with different ligand densities (Column Loading: 15 mg/mL).

Ammonium sulfate concentration (M)	Ligand density (μmol phenyl/mL drained gel)	Irreversible bound fraction ^a of aggregate species
0.35	42	0.18
0.45	42	0.20
0.35	47	0.22 ^b

^a Irreversible bound fraction was defined as $q_{2,\text{irr}}/(q_2 + q_{2,\text{irr}})$.

^b Experiment repeated one time ($n=2$) for this condition. Reported value represents the average.

two species (monomer and aggregate) possessed similar binding properties during the elution process, and the separation could be accurately predicted only if a similar binding constant was used for both species. A best fit adsorption isotherm model for the pure aggregate species (Eq. (2)) was then obtained by varying the aggregate static binding capacity constant (q_{m2}) for each of the lots at the different buffer conditions. The fraction of irreversible bound aggregate species did not significantly change over the range of elution buffer salt concentrations and adsorbent ligand densities evaluated in the studies (Table 2). Values measured for the irreversible bound aggregate fraction were within 10% over a range of operating conditions and adsorbent ligand densities. Consequently, the values used for the irreversible binding parameters ($K_{2,\text{irr}}$ and $q_{2,\text{irr}}$) in Eq. (2) for all of the adsorbent lots were the same as reported previously [22].

During the chromatographic separation, a binary mixture of monomer and aggregate is present in the liquid phase, and Eqs. (3) and (4) were used to relate the solid and liquid phases of the monomer and aggregate components [22]:

$$c_1 = \frac{q_{m2}q_1}{K_1(q_{m1}q_{m2} - q_{m2}q_1 - q_{m1}[q_2 + q_{2,\text{irr}}])} \quad (3)$$

$$c_2 = \frac{q_{m1}q_2 + K_{2,\text{irr}}q_{m1}q_2(q_{m1}q_{m2} - q_{m2}q_1 - q_{m1}[q_2 + q_{2,\text{irr}}])}{K_2(q_{m1}q_{m2} - q_{m2}q_1 - q_{m1}[q_2 + q_{2,\text{irr}}])} \quad (4)$$

3.2. Model calculations used to predict monomer and aggregate separation using packed columns

Intraparticle mass transfer was assumed to follow homogeneous diffusion for the two species (Eq. (5)) [22]:

$$\frac{\partial q_i}{\partial t} = D_{\text{eff},i} \left(\frac{\partial^2 q_i}{\partial r^2} + \frac{2}{r} \frac{\partial q_i}{\partial r} \right) \quad (5)$$

As described previously [22], homogeneous diffusion was used to describe intraparticle mass transfer instead of pore diffusion as a result of batch uptake experiments performed in separate studies with the adsorbent and the protein. In these studies, the batch uptake rate was independent of the fluid phase protein concentration over a range of initial values (0.5–2.0 mg/mL). This behavior was consistent with the homogeneous diffusion model [22], so it was selected to describe mass transfer in the modeling simulations.

The concentration (c_i) in the column for component i , as function of space (z) and time (t) can be written as

$$\tau \frac{\partial c_i}{\partial t} + L \frac{\partial c_i}{\partial z} + 3 \frac{1 - \varepsilon}{\varepsilon} \frac{k_f \tau}{R} (c_i - c_i^s) = \frac{L^2}{Pe} \frac{\partial^2 c_i}{\partial z^2} \quad (6)$$

Eqs. (5) and (6) formed a set of coupled differential equations that were solved simultaneously, under both binding and elution conditions. Eqs. (5) and (6) both required two boundary conditions to solve [22,25] which are shown in Table 3. Two initial conditions were required: (i) before column loading ($t=0$) and (ii) before protein elution ($t=t_{\text{elution}}$). Prior to column loading ($t=0$), the adsorbent and liquid phase did not contain any protein ($c_i = q_i = 0$). The concentration profile obtained in the solid and liquid phase after

Table 3
Boundary conditions for Eqs. (5) and (6) used in the modeling simulations.

Boundary	Equation
Column inlet	$\left\{ \frac{\partial c_i}{\partial z} \right\}_{(0^+, t)} = -Pe[c_i(0^-, t) - c_i(0^+, t)], \quad c_i(0^-, t) = c_{i, \text{feed}}$
Column outlet	$\left\{ \frac{\partial c_i}{\partial z} \right\}_{(z=L, t)} = 0$
Particle surface	$\left\{ \frac{\partial q_i}{\partial r} \right\}_{(r=R, t)} = \frac{k_r}{D_{\text{eff}}}(c_i - c_i^s)$
Particle center	$\left\{ \frac{\partial q_i}{\partial r} \right\}_{(r=0, t)} = 0$

the column loading and wash steps were then used as the initial conditions for the elution step ($t = t_{\text{elution}}$).

A Comsol Multiphysics software application (Comsol Multiphysics, Version 3.3) was used to solve the coupled set of differential equations using a finite element method. The system of differential equations was first approximated with a linearized model using a Newton–Raphson algorithm [26]. The discretized form of the linearized model was then solved directly using the parallel sparse direct linear solver (PARDISOL) method [27–29] in the Comsol Multiphysics software application.

After the column loading and wash steps ($t = t_{\text{elution}}$), parameters describing mass transfer and adsorption in both the solid and liquid phases were transitioned from binding to elution conditions using a sign function over a 100-s interval [30]. Following the parameter transition, elution profiles of the monomer and aggregate species were predicted by solving Eqs. (5) and (6) simultaneously. It is important to note that a decrease in the parameter transition time did not change the results of the simulations, but a finite time (>10 s) was required in order for the Comsol solver to successfully converge and complete a simulation.

4. Results and discussion

4.1. Effect of adsorbent ligand density on the equilibrium adsorption

Adsorption isotherms of the pure monomer and pure aggregate species were evaluated using the different adsorbent lots (Table 1). The isotherms of the individual species were determined under both high salt (binding conditions) (1.0 M ammonium sulfate) and low salt (elution conditions) (0.30–0.45 M ammonium sulfate) conditions.

4.1.1. Equilibrium adsorption in high salt concentrations

At high liquid phase salt concentrations (1.0 M ammonium sulfate), the monomer and aggregate species bound strongly to Phenyl Sepharose Fast Flow adsorbents, as indicated by the highly favorable isotherm. The adsorption isotherms of the different adsorbent lots were similar under binding conditions for both the monomer (Fig. 2a) and aggregate species (Fig. 2b). Differences in the adsorption among the lots containing various ligand densities (40–47 μmol phenyl/mL gel) were within experimental uncertainty. Thus, the adsorption properties of lots containing different ligand densities were indistinguishable under strongly binding (1.0 M ammonium sulfate) conditions for both the monomer and aggregate species. Since the binding properties of the examined lots were comparable, single values for the adsorption isotherm parameters (Table 4) were selected for all of the adsorbent lots, and were used in the modeling calculations (as explained in Section 3.1). It is important to emphasize that changes to the ligand density could not be detected by comparing the adsorption isotherm under strongly binding conditions, as the results show the different lots adsorbed similar amounts of both the monomer and aggregate species over the entire range of liquid phase concentrations.

Table 4

Adsorption isotherm model parameters for pure monomer (component 1) and pure aggregate (component 2) species in 1.0 M ammonium sulfate using the Phenyl Sepharose Fast Flow adsorbent lots with ligand densities ranging from 40 to 47 μmol /mL gel. Eqs. (1) and (2) were used to determine the parameters for the monomer and the aggregate species, respectively. The residual sum of squares (RSS) was defined as the average of the square of the difference between the liquid phase concentration (measured experimentally) and the liquid phase concentration predicted by the model calculations.

Parameter	Value
q_{m1} (mg/mL)	47
q_{m2} (mg/mL)	62
K_1 (mL/mg)	9.8
K_2 (mL/mg)	13.0
RSS monomer	0.33
RSS aggregate	0.15

4.1.2. Equilibrium adsorption in low salt concentrations

At lower liquid phase salt concentrations (0.30–0.45 M ammonium sulfate), the binding properties of the different lots varied significantly with the ligand density for both the monomer (Fig. 3a) and aggregate species (Fig. 3b), as illustrated by the adsorption isotherm using 0.35 M ammonium sulfate in the liquid phase. Differences in the adsorption isotherms were most pronounced for lots containing higher ligand densities (45–47 μmol phenyl/mL gel) which possessed greater binding constants (Table 5). The binding constant increased more than threefold (from 1.5 to 5.0 mL/mg) when the ligand density increased from 40 to 47 μmol phenyl/mL gel (Fig. 4).

Table 5

Adsorption isotherm model parameters for pure monomer (component 1) and pure aggregate (component 2) species in 0.30–0.45 M ammonium sulfate using Phenyl Sepharose Fast Flow adsorbent lots with ligand densities ranging from 40 to 47 μmol /mL gel. Eqs. (1) and (2) were used to determine the parameters for the monomer and the aggregate species, respectively. The residual sum of squares (RSS) was defined as the average of the square of the difference between the liquid phase concentration (measured experimentally) and the liquid phase concentration predicted by the model calculations.

Ammonium sulfate concentration (M)	Ligand density (μmol /mL)			
	40	42	45	47
0.30				
q_{m1} (mg/mL)	10.0	10.0	10.0	10.0
q_{m2} (mg/mL)	21.0	21.0	21.5	23.0
K_1 (mL/mg)	0.5	0.5	0.7	1.7
K_2 (mL/mg)	0.5	0.5	0.7	1.7
RSS monomer	0.015	0.021	0.015	0.044
RSS aggregate	0.04	0.025	0.02	0.012
0.35				
q_{m1} (mg/mL)	10.5	10.5	10.5	10.5
q_{m2} (mg/mL)	22.0	22.0	23.0	25.0
K_1 (mL/mg)	0.9	1.0	1.2	3.0
K_2 (mL/mg)	0.9	1.0	1.2	3.0
RSS monomer	0.07	0.01	0.25	0.45
RSS aggregate	0.017	0.021	0.01	0.055
0.40				
q_{m1} (mg/mL)	11.0	11.0	11.0	11.0
q_{m2} (mg/mL)	23.5	23.5	24.0	28.0
K_1 (mL/mg)	1.2	1.3	2.0	4.0
K_2 (mL/mg)	1.2	1.3	2.0	4.0
RSS monomer	0.06	0.08	0.1	0.02
RSS aggregate	0.115	0.067	0.083	0.184
0.45				
q_{m1} (mg/mL)	11.5	11.5	11.5	11.5
q_{m2} (mg/mL)	25.0	25.0	26.0	30.0
K_1 (mL/mg)	1.5	1.5	2.5	5.0
K_2 (mL/mg)	1.5	1.5	2.5	5.0
RSS monomer	0.018	0.046	0.034	2.3
RSS aggregate	0.055	0.04	0.023	0.012

For the aggregate species, a slight increase in the static capacity constant was also noted for higher ligand densities (Table 5), but the changes were much less pronounced compared with those for the binding constants. The adsorption isotherm studies also illustrated that changes to the adsorbent ligand density could be readily measured under conditions known to elute the protein mixture (0.30–0.45 M ammonium sulfate), but not under conditions in which the protein is strongly bound (1.0 M ammonium sulfate). Consequently, the separation of a mixture of monomer and aggregate species, which is dependent upon the adsorption isotherm, could potentially vary for the adsorbent lots evaluated in the study.

4.2. Effect of ligand density on monomer/aggregate separation

Separation studies using packed columns of the Phenyl Sepharose Fast Flow adsorbent lots were performed using eluate buffer salt concentrations ranging from 0.30 to 0.45 M ammonium sulfate. Ligand density had an effect on the monomer/aggregate separation using all of the evaluated conditions (Table 5), most notably at higher ligand densities. As expected, an increase in the eluate buffer salt concentration decreased both aggregate levels and yield in the eluate pool for all of the adsorbents due to a stronger hydrophobic interaction. However, at each salt concentration, adsorbent lots containing higher ligand density levels (45–47 μmol phenyl/mL gel) had lower yield and aggregate levels (Table 6). The changes in yield and aggregate levels were most severe at a ligand density of 47 μmol phenyl/mL gel. Using 0.45 M ammonium sulfate in the elution buffer, adsorbent lots containing ligand densities of 40 and 47 μmol phenyl/mL gel had yields of 80% and 58%, respectively. Similarly, aggregate levels decreased from 4.7% to 1.5% in the eluate pool with the corresponding increase in ligand density (40–47 μmol phenyl/mL gel).

Changes in the adsorption isotherm parameters, most notably the binding constant (K_i) (Table 5) were responsible for differences in the separation performance of the various lots. As discussed earlier (Section 4.1.2), a threefold increase in the binding constant was measured over the range of evaluated ligand densities (Fig. 4), which resulted in significantly lower aggregate levels and yields as the ligand density was increased. The experimental results were consistent with modeling simulation sensitivity studies performed previously [22], which predicted that yield and aggregate levels in the eluate were highly sensitive to changes in the adsorption isotherm parameters, such as the aggregate binding constant (K_2).

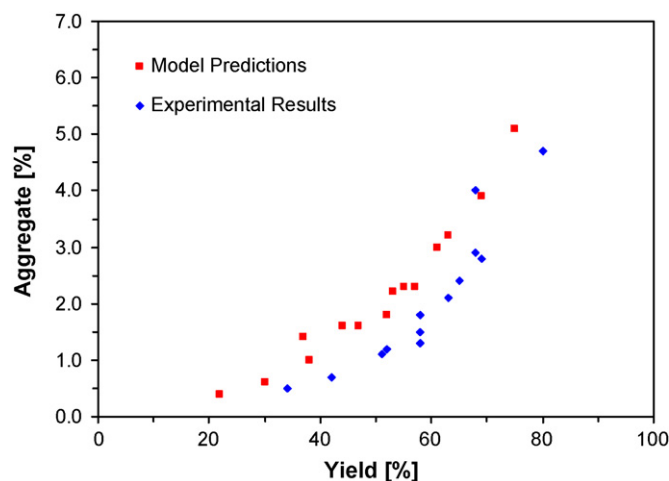


Fig. 5. Experimental results and model predictions showing the relationship between yield and aggregate levels for various Phenyl Sepharose Fast Flow adsorbent lots. The figure was generated using the results and operating conditions shown in Table 6.

4.2.1. Model predictions

Table 6 and Fig. 5 show the aggregate levels predicted by the model calculations were in good agreement with the experimental results for the adsorbent lots over a range of elution buffer salt concentrations. Differences between the model predictions and experimental results were $\leq 0.4\%$ aggregate in all cases. Model simulations slightly under predicted the yields for several of the conditions, but the trends were consistent with those measured experimentally (Fig. 5). The model predicted the largest decrease in yield and aggregate levels using an adsorbent lot containing the highest ligand density (47 μmol phenyl/mL gel), which was consistent with the experimental results (Table 6). The results of the modeling simulations showed that an increase in the binding strength, which occurred at higher ligand densities (Table 5) was a major factor for the change in separation performance for the described process. At salt concentrations used to elute the protein species (0.30–0.45 M ammonium sulfate), adsorbent lots containing higher ligand density levels (45–47 μmol phenyl/mL gel) more strongly adsorbed both monomer and aggregate species, which resulted in both lower yields and improved aggregate clearance.

Table 6

Experimental results and model predictions for separation of a monomer/aggregate mixture using Phenyl Sepharose Fast Flow adsorbents containing different ligand densities. Ammonium sulfate concentration in the Phenyl Sepharose Fast Flow elution buffer ranged from 0.30 to 0.45 M. The column was loaded to 20 mg/mL using a feed consisting of 80% monomer and 20% aggregate. The bed height and operating velocity were 20 cm and 250 cm/h, respectively. The elution volume was 6 CV.

Ammonium sulfate concentration (M)	Ligand density ($\mu\text{mol}/\text{mL}$)	Experimental results		Model predictions	
		Aggregate (%)	Yield (%)	Aggregate (%)	Yield (%)
0.30	40	–	–	5.1	75
	42	4.7	80	5.1	75
	45	4.0	68	3.9	69
	47	1.5	58	1.8	52
0.35	40	2.9	68	3.2	63
	42	2.8	69	3.0	61
	45	2.4	65	2.3	57
	47	1.1	51	1.0	38
0.40	40	–	–	2.3	55
	42	2.1	63	2.2	53
	45	1.8	58	1.6	44
	47	0.7	42	0.6	30
0.45	40	–	–	1.6	47
	42	1.3	58	1.6	47
	45	1.2	52	1.4	37
	47	0.5	34	0.4	22

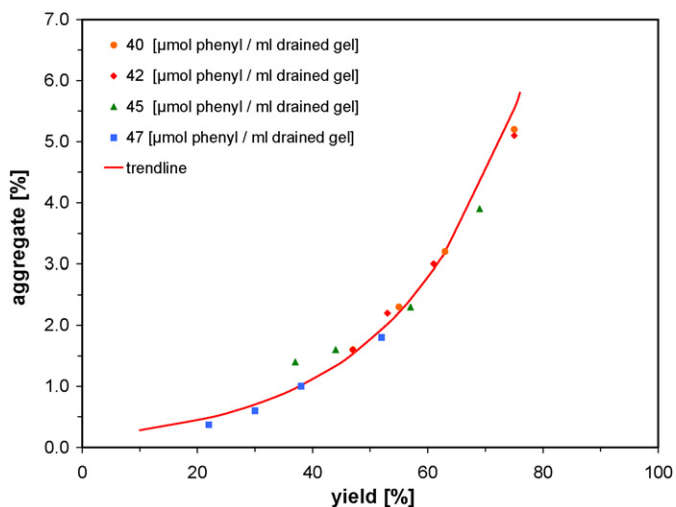


Fig. 6. Model simulations showing the relationship between yield and aggregate levels using different ammonium sulfate elution buffer conditions and various Phenyl Sepharose Fast Flow adsorbent lots in a 6 CV eluate pool. For a given adsorbent lot, aggregate levels and yields were increased by increasing the ammonium sulfate elution buffer concentration from 0.30 to 0.45 M. The column was loaded to 20 mg/mL using a feed consisting of 80% monomer and 20% aggregate in the simulations. The bed height and operating velocity were 20 cm and 250 cm/h, respectively. The solid line in the figure represents a correlation between the yield and aggregate levels predicted by the model simulations for the various adsorbent lots.

The model was used in turn to predict the effects of the eluate buffer salt concentration on the separation using different adsorbent ligand densities (Figs. 6 and 7). At a constant yield, adsorbents containing different ligand densities had similar aggregate levels if the salt concentration was adjusted to the appropriate level (Fig. 7). Figs. 6 and 7 also show that selection of a particular ligand density did not improve the separation, but rather changed the eluate buffer salt concentration required to maintain consistent levels of product yield and aggregate clearance for the Phenyl Sepharose Fast Flow column. It is important to note that changes to other operating conditions, including the protein column loading and operating velocity, also impacted the separation (product yield and aggregate clearance), as explained previously [22].

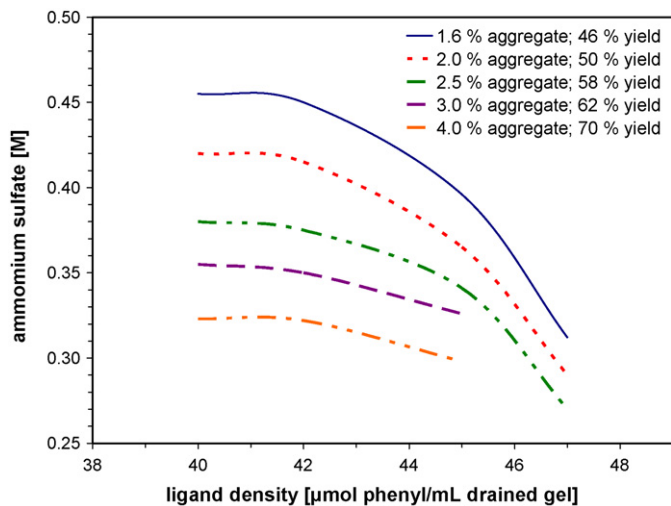


Fig. 7. Model simulations showing the effects of adsorbent ligand density and ammonium sulfate eluate buffer concentration on the yield and aggregate levels in a 6 CV eluate pool. The column was loaded to 20 mg/mL using a feed consisting of 80% monomer and 20% aggregate. The bed height and operating velocity were 20 cm and 250 cm/h, respectively.

The modeling simulations also illustrate how the eluate buffer salt concentration would need to be adjusted to reach a target aggregate level if different adsorbent lots were implemented (Fig. 7). For a lower ligand density (40–42 $\mu\text{mol phenyl/mL gel}$), the elution buffer salt concentration would have to be increased to ≥ 0.42 M ammonium sulfate to achieve aggregate levels of $\leq 2.0\%$ in the eluate pools using the examined conditions. If the ligand density was increased to 47 $\mu\text{mol phenyl/mL gel}$, a significantly lower salt concentration could be used (≥ 0.30 M ammonium sulfate) while maintaining aggregate levels $\leq 2.0\%$. Fig. 7 shows changes made to the adsorbent ligand density would require that the elution buffer conditions be significantly adjusted in order to maintain a consistent process.

In a manufacturing process which uses isocratic elution, the buffer specifications are typically set to a narrow range in order to ensure consistent product purity and recovery are achieved. In the particular separation study presented in this work, the salt concentration in the elution buffer composition would need to be significantly modified if a new adsorbent lot containing a relatively high ligand density ($>45 \mu\text{mol/mL gel}$) was implemented in the process. On the other hand, if the adsorbent ligand density was set to a fairly narrow range (such as 40–45 $\mu\text{mol/mL gel}$), a consistent purity and yield would be attained using the Phenyl Sepharose Fast Flow column without having to alter the elution buffer conditions.

5. Conclusions

Model predictions and experimental results showed changes in the separation performance (product yield and aggregate removal) of Phenyl Sepharose Fast Flow adsorbent lots containing different ligand densities were due to differences in the protein adsorption properties, as illustrated using both experimental results and modeling simulations. Differences in protein adsorption could be detected only at lower salt concentrations (0.30–0.45 M), which corresponded to the conditions used to elute the monomer/aggregate mixture. When evaluated under strongly binding (high salt) conditions (1.0 M), changes in the protein adsorption were not measurable among the different lots.

When screening lots possessing variability in the adsorbent properties, such as the ligand density, measurement of the protein adsorption isotherm for the separation of interest provides a rapid tool to predict the performance in a given chromatographic separation. However, the binding properties should be evaluated under the appropriate conditions, such as those used to elute the protein mixture, in order to detect lot to lot changes in the separation performance. The work presented here illustrates a potential alternative method of adsorbent screening, which could be used prior to selecting new adsorbent lots or lot mixtures for implementation in a manufacturing process. In a manufacturing setting, it is necessary to understand potential changes in the adsorbent properties prior to implementation in order to ensure a consistent and robust purification process is achievable.

Nomenclature

c_1	monomer concentration in solution (mg/mL)
c_2	aggregate concentration in solution (mg/mL)
CV	column volume
D_{eff}	effective diffusivity (cm^2/s) (Eq. (5))
k_f	external film mass transfer coefficient (cm/s) (Eq. (6))
K_1	monomer binding constant (mL/mg) (Eq. (1))
K_2	aggregate binding constant (mL/mg) (Eq. (2))
$K_{2,\text{irr}}$	aggregate irreversible binding constant (mL/mg) (Eq. (2))
L	bed length (cm)

Pe	Peclet number (Eq. (6))
q_1	monomer concentration in particle (bound in native state) (mg/mL) (Eq. (1))
q_2	aggregate concentration in particle (bound in native state) (mg/mL) (Eq. (2))
$q_{2,irr}$	aggregate concentration in particle (irreversible bound) (mg/mL) (Eq. (2))
$q_{m,irr}$	irreversible aggregate static capacity (mg/mL) (Eq. (2))
q_{m1}	monomer static capacity (mg/mL) (Eq. (1))
q_{m2}	aggregate static capacity (mg/mL) (Eq. (2))
r	radial coordinate (cm)
R	particle radius (cm)
t	time (s)
z	bed length coordinate (cm)

Greek symbols

ε	extraparticle void fraction (Eq. (6))
τ	fluid residence time (min) (Eq. (6))

Acknowledgements

The authors would like to thank Rich Macniven, Joshua Walker, Doug Cecchini (Biogen Idec Corporation), and Mina Sierou (Comsol, Inc.) for useful technical discussions.

References

- [1] A. Shukla, B. Hubbard, T. Tressel, S. Guhan, D. Low, J. Chromatogr. B 848 (2007) 28.
- [2] D.K. Follman, R.L. Fahrner, J. Chromatogr. A 1024 (2004) 79.
- [3] R.L. Fahrner, H.L. Knudsen, C.D. Basey, W. Galan, D. Feuerhelm, M. Vanderlaan, G.S. Blank, Biotechnol. Genet. Eng. Rev. 18 (2001) 301.
- [4] S.C. Goheen, B.M. Gibbins, J. Chromatogr. A 890 (2000) 73.
- [5] C.C. Shepard, A. Tiselius, Discussion of the Faraday Society, Hazell Watson and Winey, London, 1949, p. 275.
- [6] M.T. Hearn, in: S. Ahuja (Ed.), Handbook of Bioseparation, Academic Press, New York, 2000, p. 71.
- [7] J.A. Queiroz, C.T. Tomaz, J.M.S. Cabral, J. Biotechnol. 87 (2001) 143.
- [8] E. Boschetti, A. Jungbauer, in: S. Ahuja (Ed.), Handbook of Bioseparation, Academic Press, New York, 2000, p. 535.
- [9] G. Halperin, M. Breitenbach, M. Tauber-Finkelstein, S. Shaltiel, J. Chromatogr. 215 (1981) 211.
- [10] S. Hjerten, J. Mohammed, K.O. Eriksson, J.L. Liao, Chromatographia 31 (1991) 85.
- [11] H.P. Jennissen, A. Demiroglou, J. Chromatogr. 597 (1992) 93.
- [12] W. Schwart, D. Judd, M. Wysocki, L. Guerrier, E. Birck-Wilson, E. Boschetti, J. Chromatogr. A 908 (2001) 251.
- [13] M.T.W. Hearn, in: K.M. Gooding, F.E. Regnier (Eds.), HPLC of Biological Macromolecules, Marcel Dekker, New York, 2002, p. 99.
- [14] A. Jungbauer, W. Feng, in: K.M. Gooding, F.E. Regnier (Eds.), HPLC of Biological Macromolecules, Marcel Dekker, New York, 2002, p. 281.
- [15] S. Pahlman, J. Rosengren, S. Hjerten, J. Chromatogr. 131 (1977) 99.
- [16] J. Rosengren, S. Pahlman, M. Glad, S. Hjerten, Biochem. Biophys. Acta 412 (1975) 51.
- [17] W.R. Melander, C. Horváth, Arch. Biochem. Biophys. 183 (1977) 200.
- [18] W.R. Melander, C. Horváth, J. Chromatogr. 317 (1984) 67.
- [19] S.L. Wu, A. Figueroa, B.L. Karger, J. Chromatogr. 371 (1986) 3.
- [20] B.F. Roettger, J.A. Myers, M.R. Ladisch, F.E. Regnier, Biotechnol. Prog. 5 (1989) 79.
- [21] T.W. Perkins, D.S. Mak, T.W. Root, E.N. Lightfoot, J. Chromatogr. A 766 (1997) 1.
- [22] J.T. McCue, P. Engel, A. Ng, R. Macniven, J. Thömmes, Bioproc. Biosyst. Eng. 31 (2008) 261.
- [23] I. Langmuir, J. Am. Chem. Soc. 40 (1918) 1361.
- [24] I. Lundstrom, Prog. Colloid Polym. Sci. 70 (1985) 76.
- [25] J.T. McCue, G. Kemp, D. Low, I. Quiñones-García, J. Chromatogr. A 989 (2003) 139.
- [26] P. Deuffhard, Numer. Math. 22 (1974) 289.
- [27] O. Schenk, K. Gärtner, Parallel Comput. 28 (2002) 187.
- [28] O. Schenk, K. Gärtner, Future Gener. Comput. Syst. 20 (2004) 475.
- [29] K. Gärtner, O. Schenk, W. Fichtner, Speedup J. 12 (1999) 67.
- [30] COMSOL Multiphysics Command Reference, Version 3.3, Stockholm, 2006, p. 193.